EQA - International Journal of Environmental Quality
ISSN 2281-4485 - Vol. 70 (2025): 116-133
Journal homepage: https://eqa.unibo.it/

published by

Delineation of aquifer vulnerability to pollution: A case study in Eha Alumona, Nsukka Local Government Area, Enugu State, Nigeria

Okwudili Cornelius Ossai, Daniel Nnaemeka Obiora, Francisca Nneka Okeke, Johnson Cletus Ibuot*

[1]Department of Physics and Astronomy, University of Nigeria, Nsukka

* Corresponding author E.mail: johnson.ibuot@unn.edu.ng

Article info
Received 11/5/2025; received in revised form 7/7/2025; accepted 25/9/2025
DOI: 10.6092/issn.2281-4485/21952

Abstract
This study aims to assess the vulnerability of aquifers to contamination in Eha Alumona, Nsukka Local Government Area, Enugu State, Nigeria, using resistivity data and various vulnerability indices. The VES survey conducted across fifty stations revealed five distinct geo-electric layers, with resistivity values ranging from 5.7 to 87,620.9 Ωm, and depths varying from 0.4 to 234.5 m. The study's findings indicate that the first two layers are characterized by low resistivity values, suggesting the presence of surface materials such as sandy soil and weathered rock, which are likely to contain moisture and exhibit varying porosity. The lower layers show higher resistivity values, pointing to more consolidated or less permeable geological materials. The vulnerability assessment, based on four indices (GOD, GLSI, DRIST, and SI), reveals that the aquifer is generally low in vulnerability across the study area. The GOD index suggests low contamination risk due to deep water tables and protective layers. The GLSI and DRIST indices further indicate moderate to low susceptibility, with 62% and 64% of the study area being classified as moderately susceptible, respectively. The SI index also supports these findings, categorizing the aquifer as well-protected from contamination. Overall, the results emphasize the importance of monitoring and sustainable management practices to ensure the long-term protection of groundwater resources in the region.

Keywords: *Aquifer vulnerability, GOD index, GLSI index, DRIST index, Susceptibility Index, groundwater protection*

Introduction

The sustainable management of groundwater resources is paramount for addressing the water needs of communities, especially in regions where surface water may be limited or unreliable. In Enugu State, Nigeria, the aquifer system in the Eha-Alumona area plays a critical role in supplying water for various purposes, including domestic, agricultural, and industrial uses. However, understanding the litho-stratigraphic units, and vulnerability dynamics of the aquifer is essential for effective management and protection against potential contaminants (Ibuot et al., 2019a; Nugraha et al., 2021; Omeje et al., 2023a). Groundwater resource faces numerous threats that endanger its quality and availability. One of the most significant threats to groundwater is pollution. Groundwater pollution is becoming a significant issue globally, especially with the increasing population and industrial activities. The vulnerability of aquifers varies depending on their type, with unconfined aquifers being more susceptible to contamination than confined aquifers. Groundwater vulnerability study assesses the susceptibility of aquifers to contamination or depletion from various sources. It involves evaluating factors that influence the likelihood and potential impact of contamination, helping to prioritize areas for protection and management efforts (Rahman, 2008; George, 2020; Ibuot et al., 2017; Ibuot et al., 2019b). Assessing the vulnerability of groundwater to contamination is vital for protecting water quality. By

.

EQA 70 (2025): 116-133

DOI: 10.6092/issn.2281-4485/21952

using the electrical resistivity method, potential pathways for contaminant transport can be identified, along with areas susceptible to pollution from anthropogenic activities such as agriculture, industry, and urbanization. Anthropogenic wastes can affect groundwater quality, when these wastes can infiltrate into groundwater through pores of rock/soil on the surface of the earth that seep into groundwater repositories (Kagabu et al., 2010; Rusydi et al., 2015; Oni et al., 2017; Bakti et al., 2017; Nejatijahromi et al., 2019). According to Banerjee et al. (2023), groundwater pollution primarily results from a blend of surface and subsurface processes, which directly influence groundwater replenishment. The vulnerability of groundwater may vary due to a range of factors, including hydrogeological conditions (e.g., aquifer type, depth to water table, and permeability), land use and land cover changes, climatic conditions (e.g., precipitation and temperature variations), and anthropogenic activities (e.g., industrial discharge, agricultural practices, and urbanization), contingent upon the subsurface characteristics of a given area. These factors influencing groundwater vulnerability encompass the hydraulic conductivity of aquifer cover layers (Saravanan et al., 2018; Van Stempvoort et al., 1993; Yusuf and Abiye, 2019). Subsurface conditions can either act as a protective barrier or facilitate the transportation of pollutants, allowing them to infiltrate the aquifer layer. These protective layers serve as barriers, shielding the underlying aquifer from contaminants and pollutants that may otherwise infiltrate and degrade water quality. In vulnerability assessment, the presence and effectiveness of aquifer protective layers directly influence the rate at which contaminants can penetrate the aquifer system. Areas with robust protective layers are less vulnerable to contamination, as these layers impede the downward movement of pollutants, thereby preserving the quality of groundwater (Putranto et al. 2017, 2018). Conversely, regions lacking adequate protective layers are at higher risk of contamination, as pollutants can more easily infiltrate the aquifer and compromise its quality (Van Stempvoort et al., 1993; Obiora and Ibuot, 2020; Omeje et al., 2023b). The electrical resistivity method can be considered a quick and cost-effective methodology to estimate the general level of contaminant in groundwater (Loke 2009; Lashkaripour and Nakhaei, 2005; Ibuot et al., 2024). By monitoring changes in resistivity, the resistivity method can help assess the extent and movement of contaminants in groundwater systems (Mansour et al., 2018; Tresoldi et al., 2019). The integration of electrical resistivity techniques with indexed-based models presents a promising approach for enhancing the understanding of aquifer systems and their vulnerability to contamination. By combining geophysical data with comprehensive vulnerability assessments, researchers can develop holistic frameworks for groundwater management and protection. Furthermore, the insights gained from such integrated approaches can inform policymakers, stakeholders, and groundwater managers, facilitating sustainable use and preservation of this vital resource. The novelty of this study lies in its integrated approach to assessing aquifer vulnerability in Eha Alumona, combining resistivity data from Vertical Electrical Sounding (VES) with multiple vulnerability indices GOD (G - groundwater occurrence, O - lithological character and D - Depth to aquifer), GLSI (Geoelectric layer susceptibility index), DRIST (D-depth to groundwater, R-Net recharge, I-vadose zone's impact, S-soil media, and T-topography), and SI (Susceptibility index), a methodology not previously applied in this region. This multi-criteria evaluation will enhance the reliability of the findings, providing a comprehensive understanding of the area's subsurface geology and hydrogeological conditions. Unlike many studies that focus on a single vulnerability index, this research uses four different indices, offering a comprehensive, multi-criteria evaluation that enhances the reliability of the results. This multidisciplinary approach improves the effectiveness of groundwater management and protection strategies.Top of Form The thrust of this study is to characterize the litho-stratigraphic units and dynamics of aquifer vulnerability in Eha Alumona, Enugu State, Southeastern Nigeria using electrical resistivity method.

Location, geology and hydrogeology of the study area

The study area lies between longitude 7°26'0"E and 7°37'0"E, and latitude 6°39'0"N and 6°53'0"N (Fig. 1) Geologically, Eha-Alumona lies within the Benue Trough, which is a major geological feature extending from the Gulf of Guinea in the south to the Chad Basin in the north. The Benue Trough is known for its sedimentary rock formations, which include sandstones, shales, and limestone (Reyment 1965; Agagu et al., 1985). These sedimentary rocks have been deposited over millions of years and are associated with various geological processes such as erosion, deposition, and are often rich in fossils. The specific geological formations present in EhaAlumona and its surrounding area may include layers of sandstone, shale, and possibly li-

DOI: 10.6092/issn.2281-4485/21952

mestone (Agagu et al., 1985; Obiora and Ibuot, 2020). These geological formations influence the landscape, soil composition, and natural resources of the area. In terms of landscape, Eha-Alumona and its vicinity feature undulating terrain with hills, valleys, and occasional outcrops of rock formations (Ogbukagu 1976; Obaje 2009). The sedimentary formations often serve as aquifers, providing groundwater resources for the local population. Sandstone and fractured limestone formations can act as important water-bearing units, storing and transmitting groundwater (Obiora and Ibuot, 2020). Groundwater in Nsukka occurs in various geological formations, including weathered zones, fractured rocks, and porous sandstone layers. The depth and quality of groundwater can vary depending on the geological structure and hydrological conditions.

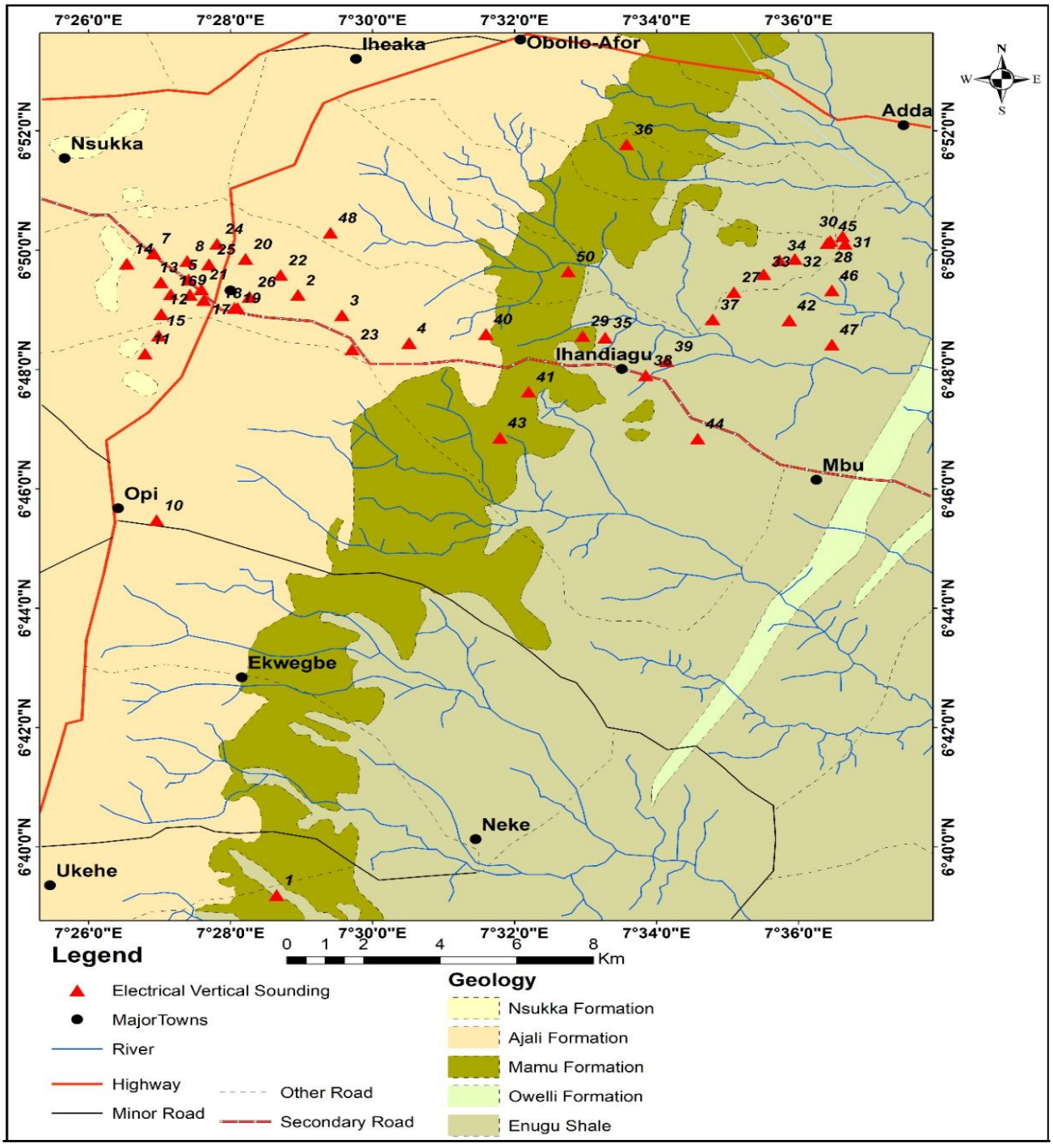

Figure 1. *Map of Eha-Alumona, Nsukka, showing the Geology and VES points*

EQA 70 (2025): 116-133

DOI: 10.6092/issn.2281-4485/21952

Methodology

Vertical Electrical Sounding (VES)

The vertical electrical sounding with the Schlumberger electrode configuration was used in this study. A profile for the study was taken along fairly straight traverses. Fifty vertical electrical soundings (VES) were taken, which translated to wider coverage of the areas earmarked for this study. The choice of the sounding points was such that it allowed for electrodes being spread along a straight traverse. At each sounding point, traverse was made by spreading a measuring tape along two opposite directions. The total traverse length for each sounding gives the maximum current electrode separation for that particular sounding. The potential difference of the subsurface was measured between the potential electrodes (M and N). The half current electrodes spread (AB/2) and half potential electrodes spread (MN/2) ranged from 1.0 m – 450.0m and 0.25 m – 20.0 m respectively. The four electrodes (A, B, M, and N) were placed in a straight line (Fig. 2), with the current electrodes (A and B) positioned far apart, and the potential electrodes (M and N) placed closer together at the center (AB ≫ MN). The maximum current electrode separation was 900 m, while the maximum potential electrode separation was 20 m. Current (I) was injected into the ground through A and B using the ABEM SAS 4000 Terrameter, and the resulting potential difference (V) between M and N was measured. To investigate deeper subsurface layers, the current electrode spacing (AB) was progressively increased while keeping the potential electrode spacing (MN) relatively small. The resistance of the subsurface were measured on the surface using the ABEM SAS 4000 Terrameter and recorded against the appropriate potential and current electrodes separation. Multiple measurements at different AB spacings generate a resistivity curve, which is analyzed to determine subsurface properties. The Global Position System (GPS) was used to measure the coordinates of the sounding points in terms of latitude and longitude as well as measuring station elevation.

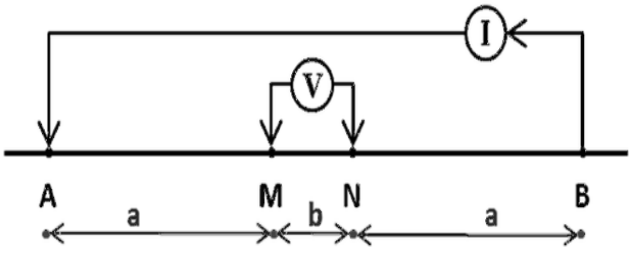

Figure 2. *Schlumberger electrode configuration*

Equation [1] was used to calculate the apparent resistivity (ρ_a).

$$\rho_a = \pi.\left[\frac{\left(\frac{AB}{2}\right)^2-\left(\frac{MN}{2}\right)^2}{MN}\right].R_a \qquad [1]$$

where $\left[\frac{\left(\frac{AB}{2}\right)^2-\left(\frac{MN}{2}\right)^2}{MN}\right]$ is the geometric factor and R_a is the apparent resistance.

The data were reduced to 1-D geological models utilising the manual and computer modelling techniques. The computed apparent resistivities were plotted against AB/2 on bi-logarithmic graphs and the curves obtained were smoothened in order to eliminate the effects of lateral heterogeneities and other forms of noisy signatures. The values of the apparent resistivity were inputted into computer software program (WinResist) for the computer modelling which generates a set of geoelectric curves from where the values of resistivity, thickness and depth of each geoelectric layer were obtained. The curves show a wide variation in values of resistivity, thicknesses and depths between and within the subsurface layers penetrated by current.

Groundwater Vulnerability Indices (GVI)

Groundwater vulnerability indices are tools used to assess the susceptibility of groundwater to contamination. These indices combine various environmental and geological factors to provide a measure of how likely groundwater is to become polluted. These indices help in the management and protection of groundwater resources by identifying areas that are more likely to be affected by contaminants. The GOD index, also known as the "GOD" vulnerability index, is a method used to assess groundwater vulnerability to pollution. This index considers geological and hydrogeological factors that influence the susceptibility of groundwater to contamination. The GOD index is determined by multiplying the effect of the three parameters, namely groundwater occurrence (G) (confined or unconfined aquifer), lithological character of the vadose zone (O) and depth to the aquifer (D). The GOD index combines these factors to provide a comprehensive assessment of groundwater vulnerability to pollution. Areas with geologically permeable formations, shallow water tables, and thin or permeable overlying lithology are likely to have higher vulnerability scores, indicating a greater risk of contamination and vice versa. This index is expressed in equation [2]. Its values range from 0 to 1 and Table 1 gives the vulnerability ranges corresponding to GOD parametric index while Table 2

DOI: 10.6092/issn.2281-4485/21952

Vulnerability class	Index rating
Negligible	0.0 – 0.1
Low	0.1 – 0.3
Moderate	0.3 – 0.5
High	0.5 – 0.7
Extreme	0.7 – 1.0

Table 1. *GOD (G - groundwater occurrence, O - lithological character and D - Depth to aquifer) parametric index rating (Foster, 1987)*

is the attribution of notes for GOD model Parameters.

$$GOD_{index} = G \times O \times D \quad [2]$$

Aquifer type	Note	Lithology (Ωm)	Note	Depth to aquifer (m)	Note
Non-aquifer	0	<60	0.4	<2	1
Artesian	0.1	60 - 100	0.5	2 – 5	0.9
Confined	0.2	100 - 300	0.7	5 – 10	0.8
Semi-confined	0.3 – 0.5	300 - 600	0.8	10 – 20	0.7
Unconfined	0.6 – 1.0	>600	0.6	20 – 50	0.6
				50 - 100	0.5

Table 2
Attribution of Notes for GOD (G - groundwater occurrence, O - lithological character and D - Depth to aquifer) model Parameters (Khemiri et al., 2013)

The geoelectric layer susceptibility index (GLSI) quantifies the protective capacity of overlying geological layers to shield groundwater from contaminants. The GLSI make use of the indices of geoelectric parameters obtained from electrical resistivity contrast of the subsurface lithology in order to assess the vulnerability of the groundwater repositories (Oni et al., 2017). By evaluating the GLSI, researchers can identify areas where groundwater is at a higher risk of contamination due to weak protective layers. This is essential for prioritizing areas for groundwater monitoring and conservation efforts (Omeje et al., 2023). In computing GLSI, we consider the ratio of the first layer resistivity index rating (ρ_{1r}), first layer thickness index rating (h_{1r}), second layer resistivity index rating (ρ_{2r}), second layer thickness index rating (h_{2r}), nth layer resistivity index rating (ρ_{nr}), the nth layer thickness index rating(h_{nr}) to the number of geo-electric layers overlying the aquifer (N), as express in equation [3]..

$$GLSI = \frac{\left[\left(\frac{\rho_{1r}+h_{1r}}{2}\right)+\left(\frac{\rho_{2r}+h_{2r}}{2}\right)+\left(\frac{\rho_{3r}+h_{3r}}{2}\right)+\cdots+\left(\frac{\rho_{nr}+h_{nr}}{2}\right)\right]}{N} \quad [3]$$

GLSI combines these factors to generate a numerical index that reflects the overall vulnerability of the groundwater system to pollution. Higher GLSI ratings indicate greater vulnerability, while lower ratings suggest lower vulnerability. Table 3 gives the rating for geoelectric layer susceptibility index for resistivity and thickness, while Table 4 gives the GLSI parametric rating.

Resistivity (Ω-m)	Lithology	Susceptibility index rating	Thickness (m)	index rating
<20	Clay/Silt	1	<2	4
20 - 50	Sandy clay	2	2 - 5	3
51 - 100	Clayey sand	3	5 - 20	2
101 - 150	Sand	4	>20	1
151 - 400	Laterite sand	2		
>400	Laterite	1		

Table 3.
Geoelectric layer susceptibility index (GLSI) rating for resistivity and Thickness (Oni et al., 2017)

Table 4. *Geoelectric layer susceptibility index (GLSI) parametric rating (Oni et al., 2017)*

Index rating	Vulnerability Class
1.0 – 1.99	Low
2.0 – 2.99	Moderate
3.0 – 3.99	High
4.0	Extreme

The DRIST index was also considered in this study, this index investigates the groundwater vulnerability by considering only parameters related to the vadose zone, unlike DRASTIC which considers the saturated zone characteristics. This vulnerability index was computed using equation [4].

$$DRIST\ Index = D_r D_w + R_r R_w + I_r I_w + S_r S_w + T_r T_w \quad [4]$$

EQA 70 (2025): 116-133

DOI: 10.6092/issn.2281-4485/21952

where D, R, I, S, and T, are the five hydrological layers, subscripts r and w signify ranking and weight. This acronym stands for D-depth to groundwater, R-Net recharge, I-vadose zone's impact, S-soil media, and T-topography. The DRIST index is calculated by assigning weights and ratings to these factors based on their relative significance to groundwater vulnerability.

The resulting score is mapped to classify areas into vulnerability categories. Each parameter is rated on a scale from 1 to 10 according to Aller et al. (1987) in DRASTIC (Depth to water table, net recharge, aquifer media, soil media, topography, impact of the vadose zone and hydraulic conductivity) model which displays the relative contamination potential of that parameter for that area (Table 5).

Table 5. *DRASTIC (depth to water table. Net recharge, aquifer media, soil media, topography, impact of the vadose zone and hydraulic conductivity) model parameters classifications, ratings (R) and weight (w) (Aller et al 1987)*

Depth of water (m)			Net Recharge			Aquifer media			Soil media			Topography (%)			Impact of vadose zone			Hydraulic conductivity (m/s)		
Interval	R	W	Interval	R	W	Interval	R	W	Interval	R	W	Interval	R	W	Interval	R	W	Interval	R	W
< 20	10	5	>0.0252	9	4	Massive Shale	2	3	Gravel	10	2	0 to 5	10	1	Gravel	10	5	9.4×10^{-4}	10	3
20 to 40	9		0.0175 – 0.0255	8		Igneous	3		Sand	9		5 to 15	8		Sand	9		4.7×10^{-4} to 9.4×10^{-4}	8	
40 to 60	7		0.0100 – 0.015	6		Glacial till	5		Laterite	8		15 to 25	6		Laterite	8		32.9×10^{-4} to 4.7×10^{-4}	6	
60 to 80	5		0.005 – 0.0103	3		Sandstone	6		Sandy Loam	6		25 to 35	4		Sandy Loam	6		14.7×10^{-4} to 32.9 $\times 10^{-4}$	4	
80 to 100	3		0.0 – 0.005	1		Limestone and shale	6		Loam	5		> 35	1		Loam Silty loam	5 4		4.7×10^{-5} to 14.75×10^{-5}	2	
100 to 120	2					Sand and gravel	8		Clay Loam	3					Clay Loam	3		4.7×10^{-7} to 4.7×10^{-5}	1	
> 120	1					Basalt	9													

Depth to water table (D) is the thickness of the vadose zone that is the distance from the ground surface to the water table. The thickness of the vadose zone act as a resistive force on the pollutants reaching the aquifer layer. When the depth to groundwater is high, the possibility of pollution is less due to higher potential for natural attenuation (Kirlas et al., 2022).

Net recharge (R) is the amount of rainwater that infiltrates through the soil and recharges the aquifer once it reaches the water table. It is a factor that provides the channel for transportation of surface pollutants into groundwater repositories.

The higher the infiltration rate the higher the pollution potential due to downward movement of pollutants (Aller et al., 1987; Kirlas et al., 2022). The net recharge was computed using Piscopo (2001) method which considers the slope, rainfall and soil permeability as express in equation [5].

$$Net\ recharge = Slope + Rainfall + Soil\ permeability \quad [5]$$

Table 6 gives the Net recharge classification, ratings and weight

Table 6. *Net recharge classification, ratings and weight (Piscopo 2001)*

Slope (%)	Rating	Soil permeability	Rating	Rainfall (mm)	Rating	Net recharge	Rating	Weight
< 2	4	Very slow	1	< 5	1	11 to 13	10	4
2 to 10	3	Slow	2	500 to 700	2	9 to 11	8	
10 to 33	2	Moderate	3	700 to 850	3	7 to 9	5	
> 33	1	Moderately	4	> 850	4	5 to 7	3	
		High	5			3 to 5	1	

DOI: 10.6092/issn.2281-4485/21952

Soil media (S) is the uppermost part of the vadose zone characterised by significant biological and chemical activities. It controls the amount of water that percolates downward into the subsurface under the influence of gravity and depends on the soil porosity and permeability and influences the flow of pollutants (Babiker et al., 2005; Ifediegwu and Chibuike 2021).

Topography (T) is the parameter that represents the slope variability of the land surface which influences the percolation of water in the subsurface. Steep slope leads to decrease in groundwater recharge and decrease in groundwater pollution while low slope will lead to high groundwater pollution (Barbulescu, 2020; Kirlas et al., 2022; Patel et al., 2022).

Vadose zone impact (I) is the unsaturated zone between the soil cover and the aquifer layer. The lithological characteristics of this zone influences the transfer of pollutants from the surface downward. It is an important component of groundwater recharge and contamination.

The Susceptibility Index (SI) is a model which considers five parameters and is an adaptation of the DRASTIC method with the omission of three parameters, namely, soil medium, unsaturated zone, and hydraulic conductivity of the aquifer. Instead, it incorporates an additional parameter, namely, land use. SI is obtained by removing S, I, and C from DRASTIC and including the land use parameter (LU) that incorporates the agricultural activities' impact on the water quality (Stigter et al., 2006). In recent studies, the integration of the land use factor in the assessment of groundwater quality is a key issue that should be considered in predicting the effect of anthropogenic activities on groundwater quality (Brindha and Elango, 2015; Teixeira et al., 2015). Similar to the DRASTIC and GOD methods, the SI approach was developed to assess the vulnerability of aquifers on large and medium scales, and is calculated using equation 6.

$$SI = D_r D_w + R_r R_w + A_r A_w + T_r T_w + LU_r LU_w \qquad [6]$$

where D, R, A, T, and Lu, are the five hydrological layers, subscripts r and w signify ranking and weight. This acronym stands for D-depth to groundwater, R-Net recharge, A-Aquifer media, T-Topography, and LU-Land use. The SI is calculated as a weighted sum of these parameters, providing a composite score that classifies areas into different vulnerability levels (e.g., low, moderate, high). The index is widely applied in groundwater management to identify areas at risk, prioritize monitoring, and guide sustainable land-use planning.

The parameters' weights are: D_w = 0.185, R_w = 0.212, A_w = 0.259, T_w = 0.121, LU_w = 0.222.

Table 7 will be used in the classification of the DRIST and SI vulnerability indices'.

Table 7. *Vulnerability assessment criteria for DRIST (depth to water table, net recharge, impact of the vadose zone, soil media and topography) and SI (susceptibility index) methods (Corniello et al., 1997; Foster, 1998; Rebeiro, 2000)*

	DRIST	SI
Very low	<80	---
Low	80 – 120	<45
Moderate	121 – 160	45 – 64
High	161 – 200	65 – 85
Very high	>200	>85

Results and Discussion

Vertical Electrical Sounding (VES)

The presented Vertical Electrical Sounding (VES) result (Table 8) shows varying values of geoelectric layers resistivity, thickness and depth from fifty VES stations, providing insight into subsurface characteristics across the surveyed area. Five geo-electric layers were delineated from the 50 VES points across the study area within the maximum current electrode spread. The first two layers generally show lower resistivity values, ranging from 5.7 Ωm – 767.2 Ωm with thickness and depth ranging from 0.4 m – 3.5 m in layer 1, while layer 2 has resistivity values ranging from 7.2 Ωm– 5507.6 Ωm with its thickness and depth ranging from 1.3 m – 17.9 m and 3.4 m – 19.3 m respectively. These resistivities could indicate surface materials like sandy soil, clay, or weathered rock, which have relatively high moisture content and porosity, while the range of the thickness of layers 1 and 2 suggests variability in the thickness of weathered or less consolidated surface materials. The third geo-electric layer is characterized by resistivity values ranging 10.6 Ωm – 4656.9 Ωm. The thickness and depth of this layer range from 5.7 m – 52.1 m, and 10.3 m to 67.6 m respectively. The fourth layer is characterized by resistivity values ranging from 31.4 Ωm – 9806.3 Ωm with thickness and depth ranging from 13.8 m – 180.9 m, and 25.8 m – 234.5 m respectively. The fifth layer resistivity values range from 2.6 Ωm– 87620.9 Ωm with thickness and depth undefined within the maximum current electrode separation. The variations in these parameters may be due to factors such as geological composition, porosi-

DOI: 10.6092/issn.2281-4485/21952

Table 8: *Result of interpreted geoelectric data (ρ - resistivity, h - thickness, d - depth)*

VES No.	Long. (°E)	Lat. (°N)	Elevation (m)	Layer Resistivity (Ωm)					Layer thickness (m)				Layer depth (m)			
				ρ_1	ρ_2	ρ_3	ρ_4	ρ_5	h_1	h_2	h_3	h_4	d_1	d_2	d_3	d_4
1	7.4751	6.6221	477	47.2	343.8	37.0	179.2	2057.8	1.5	8.7	24.9	23.1	1.5	10.2	35.1	58.2
2	7.4825	6.8208	435	76.2	32.2	888.2	1487.8	15202.5	2.0	6.7	9.5	102.2	2.0	8.7	18.2	120.3
3	7.4928	6.8152	416	264.7	5389.7	2196.5	9728.1	34426.8	0.6	5.6	27.9	33.3	0.6	6.2	34.1	67.4
4	7.5086	6.8074	345	419.9	1996.3	667.0	48.7	782.7	0.7	7.1	19.9	68.8	0.7	7.8	27.7	96.5
5	7.4568	6.8251	498	9.8	1053.2	674.6	1538.3	1765.3	0.5	5.7	27.6	68.4	0.5	6.2	33.8	102.2
6	7.4389	6.5091	474	128.8	452.3	3189.1	1131.6	7628.9	3.1	1.3	33.1	60.1	3.1	4.4	35.5	97.6
7	7.4486	6.8325	491	123.9	470.2	2061.4	3578.1	152.7	0.6	11.8	22.5	68.4	0.6	12.4	34.8	103.2
8	7.4565	6.8303	485	127.4	4827.4	403.3	7609.9	4689.6	0.5	2.9	11.1	68.5	0.5	3.4	14.5	82.9
9	7.4571	6.8209	504	384.5	106.2	1178.8	3771.5	28432.6	3.2	4.9	14.2	30.5	3.2	8.1	22.2	52.7
10	7.4493	6.7579	505	168.2	1403.1	599.0	2401.4	5083.9	0.5	3.4	38.7	139.8	0.5	3.9	42.6	182.3
11	7.4466	6.8044	517	667.1	909.2	2565.5	6942.0	9925.5	2.3	12.6	19.3	59.7	2.3	14.9	34.2	94
12	7.4504	6.8155	504	263.3	563.8	2868.2	4021.4	5457.7	0.5	14.9	52.1	146.3	0.5	15.5	67.6	213.8
13	7.4503	6.8244	524	261.3	4240.2	1838.9	9806.3	991.7	0.4	4.5	17.3	91.9	0.4	4.9	22.1	114
14	7.4423	6.8296	477	220.8	11.9	605.6	6205.7	607.1	1.6	2.9	5.8	116.4	1.6	4.5	10.3	126.6
15	7.4498	6.8095	500	101.6	3230.3	626.7	4240.2	2277.1	0.4	5.0	21.2	44.9	0.4	5.4	26.6	71.5
16	7.4526	6.8210	519	166.7	54.5	1302.3	6419.5	87620.9	2.2	4.2	5.7	13.8	2.2	6.4	12.0	25.8
17	7.4604	6.8194	501	23.0	596.5	1629.8	8065.1	21682.6	0.5	10.7	12.2	38.2	0.5	11.2	23.4	61.6
18	7.4683	6.8172	506	131.5	180.4	4049.5	1298.4	2473.6	3.0	2.3	30.2	165.7	3.0	5.3	35.5	201.2
19	7.4676	6.8172	470	24.0	437.5	242.1	2328.2	101.5	0.5	6.9	13.5	66.4	0.5	7.4	20.9	87.2
20	7.4702	6.8309	476	36.2	108.5	487.3	645.2	68.8	1.5	9.1	35.4	77.5	1.5	10.6	46.0	123.5
21	7.4598	6.8224	494	112.7	710.1	269.5	8398.7	4787.3	1.0	6.6	16.2	88.7	1.0	7.6	23.7	112.4
22	7.4784	6.8264	508	558.5	584.6	1294.9	1560.9	1013.4	1.5	17.9	35.8	111.1	1.5	19.3	55.1	166.2
23	7.4952	6.8056	533	5.7	46.2	177.3	948.2	19850.1	0.7	9.5	8.1	15.2	0.7	10.2	18.3	33.5
24	7.4635	6.8351	462	19.0	63.9	618.6	2182.5	18103.5	3.5	2.2	8.9	19.2	3.5	5.7	14.6	33.8
25	7.4616	6.8294	493	36.4	62.6	255.1	867.8	109.1	1.2	6.9	26.6	83.0	1.2	8.0	34.6	117.6
26	7.4711	6.8203	491	32.8	25.6	327.5	982.9	224.3	3.0	6.1	13.8	87.4	3.0	9.1	22.9	110.3
27	7.5848	6.8216	229	83.8	13.8	119.0	1526.3	193.5	2.4	6.0	8.5	88.0	2.4	8.4	16.9	104.9
28	7.6068	6.8354	240	68.7	14.2	208.5	417.1	15.0	2.7	6.4	14.0	49.6	2.7	9.2	23.1	72.7
29	7.5493	6.8094	242	21.1	74.5	23.7	1517.5	811.7	2.0	6.4	15.4	100.0	2.0	8.3	23.7	123.7
30	7.6103	6.8372	233	19.0	47.8	60.0	85.0	564.6	2.7	8.0	28.2	54.8	2.7	10.7	38.9	93.7
31	7.6109	6.8351	230	34.8	80.4	23.2	147.6	14.8	1.2	5.5	18.2	68.9	1.2	6.6	24.9	93.7
32	7.5991	6.8309	241	240.9	147.2	10.6	261.5	1580.7	2.0	6.1	25.1	48.5	2.0	8.1	33.2	81.7
33	7.5918	6.8266	221	145.6	115.1	24.6	183.2	1899.9	1.5	5.9	17.9	56.0	1.5	7.4	25.2	81.2
34	7.5955	6.8305	241	199.9	278.3	358.5	159.6	149.1	2.3	7.0	44.2	180.9	2.3	9.4	53.6	234.5
35	7.5546	6.8089	234	89.9	7.2	27.7	31.4	2.6	1.9	5.8	35.7	65.8	1.9	7.8	43.4	109.3
36	7.5596	6.8629	252	160.1	70.3	25.1	2156.0	2463.3	2.1	5.2	16.2	69.2	2.1	7.3	23.5	92.7
37	7.5798	6.8140	192	602.4	74.8	107.5	2768.3	25358.1	2.8	4.3	17.5	36.9	2.8	7.1	24.6	61.5
38	7.5641	6.7984	248	55.5	98.1	100.1	758.7	6646.2	1.5	2.4	8.5	23.4	1.5	3.9	12.4	35.8
39	7.5690	6.8023	237	90.9	10.6	39.3	163.5	221.1	1.8	12.0	9.0	41.6	1.8	13.7	22.7	64.3
40	7.5266	6.8099	301	371.5	82.8	617.3	324.2	8998.9	2.2	4.0	25.2	31.4	2.2	6.2	45.7	77.2
41	7.5366	6.7938	253	44.1	35.8	333.0	1313.8	65.0	3.0	6.5	15.4	33.6	3.0	9.5	24.9	91.7
42	7.5978	6.8138	315	279.2	5507.6	2520.8	9537.2	36300.9	0.6	5.9	29.9	33.6	0.6	6.4	36.4	69.9
43	7.5299	6.7810	264	10.3	977.3	766.1	1359.2	2001.5	0.5	5.9	28.4	70.3	0.5	6.4	34.8	105.1
44	7.5763	6.7807	243	442.3	122.1	1355.4	4336.8	32697.5	3.2	4.9	14.2	30.5	3.2	8.1	22.2	52.7
45	7.6074	6.8359	305	767.2	1045.8	2938.6	8005.8	11456.4	2.3	12.6	19.3	59.6	2.3	14.9	34.2	93.8
46	7.6078	6.8221	289	151.2	207.4	4656.9	1493.2	2844.7	3.0	2.3	30.2	165.7	3.0	5.3	35.5	201.2
47	7.6078	6.8070	212	41.6	124.7	555.4	742.6	79.2	1.5	9.0	35.4	77.6	1.5	10.5	45.9	123.6
48	7.4901	6.8382	324	642.1	672.4	1488.7	1792.2	1167.3	1.5	17.8	35.9	111.1	1.5	19.3	55.2	166.3
49	7.6055	6.8975	238	39.4	92.6	26.9	176.7	14.0	1.1	5.5	18.5	67.5	1.1	6.6	25.1	92.6
50	7.5459	6.8274	226	26.7	109.3	291.1	1189.8	4198.0	2.0	5.8	14.6	37.1	2.0	7.8	22.4	59.5

ty, permeability, anthropogenic factors, geochemical processes etc. The spatial variation of these parameters reflects the inhomogeneity of the subsurface geologic materials.

Vulnerability Indices

GOD Index. The estimated values of the GOD index (Table 9) ranged from 0.12 – 0.24, this index classified the vulnerability of the entire study area as low. The values may be influenced by the individual GOD parameters (Oni et al., 2017). This result is similar to the results Eyankware et al. (2020) and Omeje et al. (2023a) whose studies delineated the vulnerability of their study area as low. The low vulnerability classification suggests that the aquifer is less susceptible to contamination due to factors like; significant depth to the water table, which provides a buffer for conta--minant attenuation. Overlying impermeable or semi-impermeable layers that restrict the downward movement of contaminants. The aquifer likely has natural barriers, such as; thick, low-permeability vadose zone layers. Also, confined or semi-confined conditions that shield the aquifer from surface influences. These conditions reduce the potential for rapid infiltration and migration of contaminants. Although the vulnerability is low, contamination can still occur, especially from persistent or highly mobile pollutants such as nitrate, pesticides etc. Preventive measures are essential to maintain water quality over the long term. The variation of GOD index is shown in Figure 2.

DOI: 10.6092/issn.2281-4485/21952

Table 9. *Summary of aquifer vulnerability using GOD parametric model*

VES points	Longitude (°E)	Latitude (°N)	Vulnerability indices			GOD Index	Vulnerability class
			G	O	D		
1	7.4751	6.6221	0.6	0.4	0.5	0.12	Low
2	7.4825	6.8208	0.6	0.5	0.5	0.15	Low
3	7.4928	6.8152	0.6	0.6	0.5	0.18	Low
4	7.5086	6.8074	0.6	0.6	0.5	0.18	Low
5	7.4568	6.8251	0.6	0.6	0.5	0.18	Low
6	7.4389	6.5091	0.6	0.6	0.5	0.18	Low
7	7.4486	6.8325	0.6	0.6	0.5	0.18	Low
8	7.4565	6.8303	0.6	0.6	0.5	0.18	Low
9	7.4571	6.8209	0.6	0.6	0.5	0.18	Low
10	7.4493	6.7579	0.6	0.6	0.5	0.18	Low
11	7.4466	6.8044	0.6	0.6	0.5	0.18	Low
12	7.4504	6.8155	0.6	0.6	0.5	0.18	Low
13	7.4503	6.8244	0.6	0.6	0.5	0.18	Low
14	7.4423	6.8296	0.6	0.6	0.5	0.18	Low
15	7.4498	6.8095	0.6	0.6	0.5	0.18	Low
16	7.4526	6.8210	0.6	0.6	0.6	0.22	Low
17	7.4604	6.8194	0.6	0.6	0.5	0.18	Low
18	7.4683	6.8172	0.6	0.6	0.5	0.18	Low
19	7.4676	6.8172	0.6	0.8	0.5	0.24	Low
20	7.4702	6.8309	0.6	0.8	0.5	0.24	Low
21	7.4598	6.8224	0.6	0.6	0.5	0.18	Low
22	7.4784	6.8264	0.6	0.6	0.5	0.18	Low
23	7.4952	6.8056	0.6	0.7	0.5	0.21	Low
24	7.4635	6.8351	0.6	0.6	0.5	0.18	Low
25	7.4616	6.8294	0.6	0.7	0.5	0.21	Low
26	7.4711	6.8203	0.6	0.8	0.5	0.24	Low
27	7.5848	6.8216	0.6	0.5	0.5	0.15	Low
28	7.6068	6.8354	0.6	0.4	0.5	0.12	Low
29	7.5493	6.8094	0.6	0.4	0.5	0.12	Low
30	7.6103	6.8372	0.6	0.4	0.5	0.12	Low
31	7.6109	6.8351	0.6	0.4	0.5	0.12	Low
32	7.5991	6.8309	0.6	0.7	0.5	0.21	Low
33	7.5918	6.8266	0.6	0.7	0.5	0.21	Low
34	7.5955	6.8305	0.6	0.8	0.5	0.24	Low
35	7.5546	6.8089	0.6	0.4	0.6	0.14	Low
36	7.5596	6.8629	0.6	0.5	0.6	0.18	Low
37	7.5798	6.8140	0.6	0.6	0.5	0.18	Low
38	7.5641	6.7984	0.6	0.4	0.6	0.14	Low
39	7.5690	6.8023	0.6	0.4	0.5	0.12	Low
40	7.5266	6.8099	0.6	0.6	0.5	0.18	Low
41	7.5366	6.7938	0.6	0.8	0.5	0.24	Low
42	7.5978	6.8138	0.6	0.6	0.5	0.18	Low
43	7.5299	6.7810	0.6	0.6	0.5	0.18	Low
44	7.5763	6.7807	0.6	0.6	0.5	0.18	Low
45	7.6074	6.8359	0.6	0.6	0.5	0.18	Low
46	7.6078	6.8221	0.6	0.8	0.5	0.24	Low
47	7.6078	6.8070	0.6	0.7	0.5	0.21	Low
48	7.4901	6.8382	0.6	0.6	0.5	0.18	Low
49	7.6055	6.8975	0.6	0.4	0.5	0.12	Low
50	7.5459	6.8274	0.6	0.7	0.5	0.21	Low

EQA 70 (2025): 116-133

DOI: 10.6092/issn.2281-4485/21952

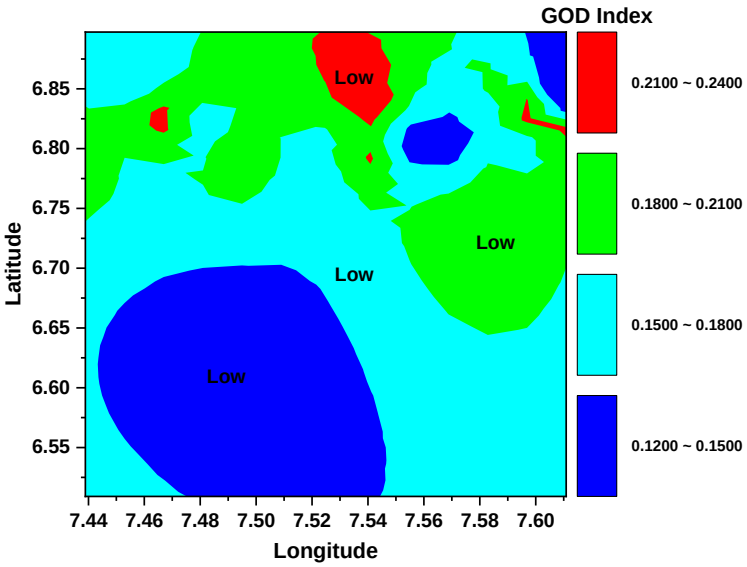

Figure 2. *Contour map showing the GOD index*

Geo-electric Layer Susceptibility Index (GLSI). This index classifies the study area into low and moderate which presented in Table 10, the GLSI vulnerability index ranged from 1.33 to 2.67 and falls with the ranged obtained bt Omeje et al. (2023a). This result delineated greater part of the study area as moderately vulnerable similar to the study of Omeje et al. (2023a) and Oni et al. (2017). The low susceptibility areas with values ranging from 1.33 to 2.67 indicate that the overlying geological layers have a high protective capacity (Oni et al., 2017). These areas may likely be dominated by materials such as clay or compacted soil, which reduce the risk of contaminants reaching the aquifer. Groundwater in these areas is relatively less vulnerable to contamination from surface activities. The moderate susceptibility areas with values ranging from 2.00 to 2.67 indicate that the protective capacity of the overlying geological layers is moderate meaning contaminants have a higher chance of penetrating to the aquifer compared to low-susceptibility zones. The subsurface materials might include a mix of clay, silt, and sand, offering intermediate protection. Low susceptibility areas could be prioritized for high-risk activities due to the natural protective barrier, but only if they comply with sustainable groundwater use practices. Moderate susceptibility areas should have stricter zoning regulations, ensuring activities with high contamination potential are avoided or mitigated. The contour map of Figure 3a shows areas with low susceptibility in the northeastern part while the greater parts have moderate susceptibility. Figure 3b is pie chart showing the percentage distribution of GLSI index, where 62 % is moderately susceptible to contamination while 38 % is low.

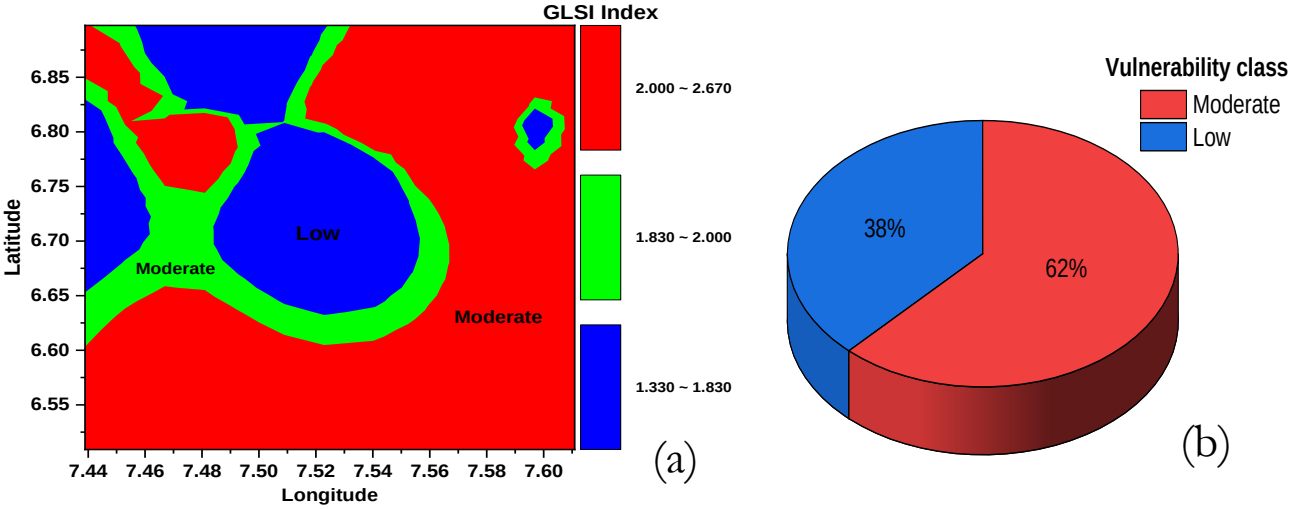

Figure 3. (a) *Contour map showing the GLSI index*; (b) *Percentage distribution of GLSI index*

EQA 70 (2025): 116-133

DOI: 10.6092/issn.2281-4485/21952

Table 10: Summary of aquifer vulnerability using GLSI parametric model

VES points	Longitude (°E)	Latitude (°N)	$\frac{(\rho_{1r}+h_{1r})}{2}$	$\frac{(\rho_{2r}+h_{2r})}{2}$	$\frac{(\rho_{3r}+h_{3r})}{2}$	GLSI Index	Vulnerability class
1	7.4751	6.6221	3	2	1.5	2.17	Moderate
2	7.4825	6.8208	3	2	1.5	2.17	Moderate
3	7.4928	6.8152	3	1.5	1	1.83	Low
4	7.5086	6.8074	2.5	1.5	1.5	1.83	Low
5	7.4568	6.8251	1.5	1.5	1	1.33	Low
6	7.4389	6.5091	3.5	1.5	1.5	2.17	Moderate
7	7.4486	6.8325	3	1.5	1	1.83	Low
8	7.4565	6.8303	3	2	1.5	2.17	Moderate
9	7.4571	6.8209	2.5	3.5	1.5	2.50	Moderate
10	7.4493	6.7579	2	2	1	1.67	Low
11	7.4466	6.8044	2	1.5	1.5	1.67	Low
12	7.4504	6.8155	2	1.5	1	1.50	Low
13	7.4503	6.8244	2	2	1.5	1.83	Low
14	7.4423	6.8296	2	2	1.5	1.83	Low
15	7.4498	6.8095	3	1.5	1	1.83	Low
16	7.4526	6.8210	2.5	3	1.5	2.33	Moderate
17	7.4604	6.8194	2	1.5	1.5	1.67	Low
18	7.4683	6.8172	3.5	2.5	1	2.33	Moderate
19	7.4676	6.8172	2	1.5	2	1.83	Low
20	7.4702	6.8309	2	3	1	2.00	Moderate
21	7.4598	6.8224	3	1.5	2	2.17	Moderate
22	7.4784	6.8264	1.5	1.5	1	1.33	Low
23	7.4952	6.8056	1.5	2	2	1.83	Low
24	7.4635	6.8351	2	2.5	1.5	2.00	Moderate
25	7.4616	6.8294	2	2.5	1.5	2.00	Moderate
26	7.4711	6.8203	2.5	2	2	2.17	Low
27	7.5848	6.8216	3	1.5	3	2.50	Moderate
28	7.6068	6.8354	3	1.5	2	2.17	Moderate
29	7.5493	6.8094	2.5	2.5	2	2.33	Moderate
30	7.6103	6.8372	2	2	2	2.00	Moderate
31	7.6109	6.8351	2	2.5	2	2.17	Moderate
32	7.5991	6.8309	2	3	1	2.00	Moderate
33	7.5918	6.8266	3	3	2	2.67	Moderate
34	7.5955	6.8305	2.5	2	1.5	2.00	Moderate
35	7.5546	6.8089	2.5	1.5	2	2.00	Moderate
36	7.5596	6.8629	2.5	2.5	2	2.33	Moderate
37	7.5798	6.8140	2	3	3	2.67	Moderate
38	7.5641	6.7984	2.5	3	1.5	2.33	Moderate
39	7.5690	6.8023	2.5	1.5	2	2.00	Moderate
40	7.5266	6.8099	2.5	3	1	2.17	Moderate
41	7.5366	6.7938	2.5	2	2	2.17	Moderate
42	7.5978	6.8138	2	1.5	1	1.50	Low
43	7.5299	6.7810	1.5	1.5	1	1.33	Low
44	7.5763	6.7807	2	3.5	1.5	2.33	Moderate
45	7.6074	6.8359	2	1.5	1.5	1.67	Low
46	7.6078	6.8221	2.5	2.5	1	2.00	Moderate
47	7.6078	6.8070	2	3	1	2.00	Moderate
48	7.4901	6.8382	1.5	1.5	1	1.33	Low
49	7.6055	6.8975	2	2.5	2	2.17	Moderate
50	7.5459	6.8274	2	3	2	2.33	Moderate

DOI: 10.6092/issn.2281-4485/21952

DRIST Index. The DRIST index with values ranging from 89 - 143 also classifies the study area into low and moderate as presented in Table 11. The low vulnerability areas are areas that are relatively well-protected from contamination due to factors like deeper water tables, low recharge rates, or protective soil and geological layers. Pollutants are less likely to reach the aquifer, even under stress from human activities. In the low vulnerability areas, the subsurface materials may include thick, impermeable layers such as clay, compacted soils, or dense rock. These materials act as natural barriers, slowing or preventing the downward movement of contaminants. The moderate vulnerability areas are areas that are at higher risk of contamination than the low vulnerability areas. Contaminants could potentially reach the aquifer depending on local conditions like soil permeability, recharge intensity, or slope gradients. In moderate vulnerability areas, the subsurface materials in these areas may include moderately permeable soils, such as sandy loam or fractured rock. These materials allow some infiltration of water and contaminants, increasing the risk of groundwater pollution. In the low vulnerability areas, regular groundwater quality monitoring can be less frequent but should remain part of the overall resource management strategy. In the moderate vulnerability areas, intensive monitoring programs should be established to track potential contamination sources and groundwater quality trends. Early detection of contamination is key to implementing timely remediation measures. The variation of DRIST index is illustrated in the contour map of Figure 4a where low vulnerability is observed in the northeastern and southwestern part of the study area. Figure 4b is a pie chart showing the percentage distribution DRIST where 64 % of the study area represents. the low vulnerability areas while 36 % represents the moderate vulnerability areas.

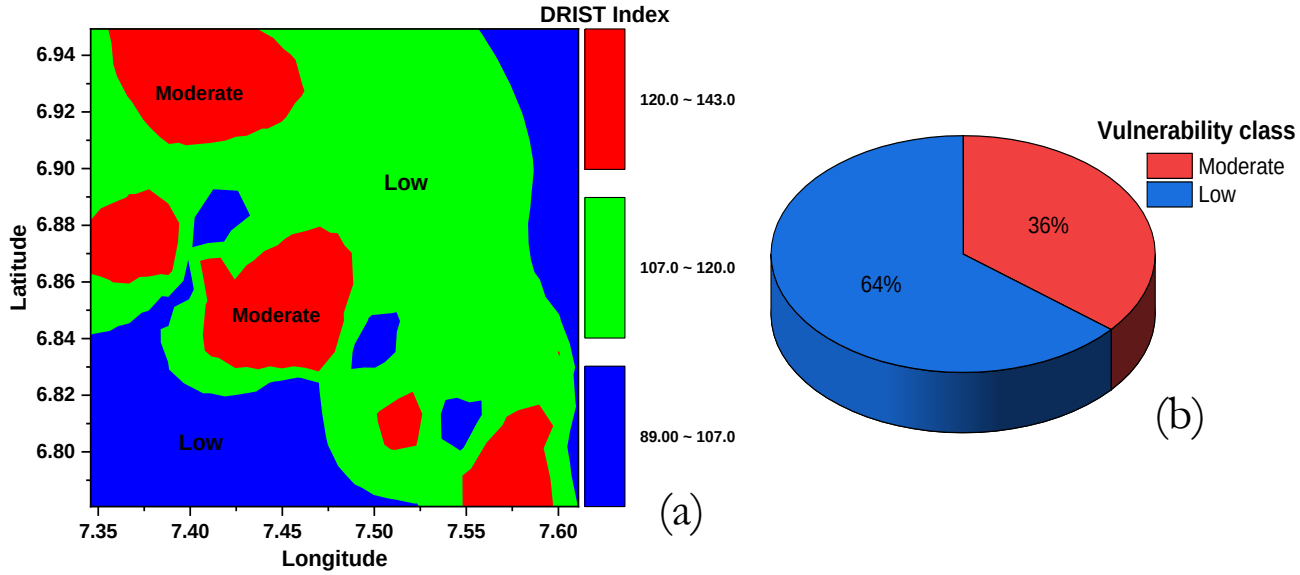

Figure 4. (a) *Contour map showing the variation DRIST index*; (b) *Percentage distribution of DRIST index*

Susceptibility Index (SI). The SI index whose values range from 15.503 – 17.373 classifies the study area into low vulnerability and the result is presented in Table 12. This is contrary to the results of Ghouili et al. (2021) who delineated 90% of their study as moderately vulnerable and Hilal et al. (2024) whose results delineated 70% of their study area as moderately vulnerable while 3% and 26% as low and high respectively. This implies that the aquifer in the study area is well-protected from contamination due to favourable conditions such as deep-water table, impermeable soil layers, or low recharge rates. This may be attributed to subsurface materials such as clay, silt, or compacted soils which have low permeability, reducing the rate at which water and contaminants percolate downward. Also, the thick vadose zone or substantial layers of impermeable material provide greater resistance to contaminant movement, effective-

DOI: 10.6092/issn.2281-4485/21952

Table 11. *Summary of aquifer vulnerability using DRIST model*

	Longitude (°E)	Latitude (°N)	5		4		5		2		1		DRIST Vulnerability Index (DVI)	Vulnerability Class (VC)
			D_r	$5D_r$	R_r	$4R_r$	I_r	$5I_r$	S_r	$2S_r$	T_r	$1T_r$		
1	7.4222	6.8525	7	35	8	32	8	40	8	16	10	10	133	Moderate
2	7.4098	6.8596	1	5	8	32	8	40	8	16	10	10	103	Low
3	7.4127	6.8693	5	25	8	32	8	40	8	16	10	10	123	Moderate
4	7.4231	6.8613	2	10	8	32	9	45	9	18	10	10	115	Low
5	7.3843	6.8634	3	15	8	32	9	45	9	18	8	8	118	Low
6	7.4267	6.8613	3	15	8	32	9	45	9	18	10	10	120	Moderate
7	7.4079	6.8691	3	15	8	32	9	45	9	18	10	10	120	Moderate
8	7.3586	6.8948	3	15	8	32	8	40	8	16	10	10	113	Low
9	7.4065	6.9247	7	35	8	32	8	40	8	16	8	8	131	Moderate
10	7.4089	6.8698	1	5	8	32	9	45	9	18	8	8	108	Low
11	7.4065	6.8585	3	15	8	32	9	45	9	18	8	8	118	Low
12	7.4056	6.8681	1	5	8	32	8	40	8	16	8	8	101	Low
13	7.4123	6.8716	2	10	8	32	8	40	8	16	8	8	106	Low
14	7.4038	6.8719	1	5	8	32	8	40	8	16	10	10	103	Low
15	7.4275	6.9493	5	25	8	32	8	40	8	16	8	8	121	Moderate
16	7.4105	6.8651	9	45	8	32	8	40	8	16	8	8	141	Moderate
17	7.4016	6.8589	5	25	3	12	8	40	8	16	8	8	101	Low
18	7.4091	6.8625	1	5	8	32	8	40	8	16	8	8	101	Low
19	7.4132	6.8639	3	15	8	32	8	40	8	16	10	10	113	Low
20	7.3980	6.8617	1	5	8	32	8	40	8	16	10	10	103	Low
21	7.4067	6.8696	2	10	8	32	8	40	8	16	10	10	108	Low
22	7.3459	6.8170	1	5	8	32	8	40	8	16	8	8	101	Low
23	7.3863	6.8676	9	45	8	32	8	40	8	16	8	8	141	Moderate
24	7.4635	6.8351	9	45	8	32	8	40	8	16	10	10	143	Moderate
25	7.4616	6.8294	2	10	8	32	8	40	8	16	10	10	108	Low
26	7.4711	6.8203	2	10	8	32	8	40	8	16	10	10	108	Low
27	7.5848	6.8216	2	10	8	32	8	40	8	16	10	10	108	Low
28	7.6068	6.8354	5	25	8	32	8	40	8	16	10	10	123	Moderate
29	7.5493	6.8094	1	5	8	32	6	30	6	12	10	10	89	Low
30	7.6103	6.8372	3	15	8	32	6	30	6	12	10	10	99	Low
31	7.6109	6.8351	3	15	8	32	6	30	6	12	10	10	99	Low
32	7.5991	6.8309	3	15	8	32	8	40	8	16	10	10	113	Low
33	7.5918	6.8266	3	15	8	32	8	40	8	16	10	10	113	Low
34	7.5955	6.8305	1	5	8	32	8	40	8	16	10	10	103	Low
35	7.5546	6.8089	2	10	8	32	8	40	8	16	10	10	108	Low
36	7.5596	6.8629	3	15	8	32	8	40	8	16	10	10	113	Low
37	7.5798	6.8140	5	25	8	32	8	40	8	16	10	10	123	Moderate
38	7.5641	6.7984	9	45	8	32	6	30	6	12	10	10	129	Moderate
39	7.5690	6.8023	5	25	8	32	8	40	8	16	10	10	123	Moderate
40	7.5266	6.8099	5	25	8	32	8	40	8	16	10	10	123	Moderate
41	7.5366	6.7938	3	15	8	32	8	40	8	16	10	10	113	Moderate
42	7.5978	6.8138	5	25	8	32	8	40	8	16	10	10	123	Moderate
43	7.5299	6.7810	2	10	8	32	8	40	8	16	10	10	108	Low
44	7.5763	6.7807	7	35	8	32	8	40	8	16	10	10	133	Moderate
45	7.6074	6.8359	3	15	8	32	9	45	9	18	10	10	120	Moderate
46	7.6078	6.8221	1	5	8	32	9	45	9	18	10	10	110	Low
47	7.6078	6.8070	1	5	8	32	8	40	8	16	10	10	103	Low
48	7.4901	6.8382	1	5	8	32	8	40	8	16	10	10	103	Low
49	7.6055	6.8975	3	15	8	32	6	30	6	12	10	10	99	Low
50	7.5459	6.8274	7	35	8	32	6	30	6	12	10	10	119	Low

DOI: 10.6092/issn.2281-4485/21952

Table 12. *Summary of aquifer vulnerability using Susceptibility Index (SI) model*

	Longitude	Latitude	0.185		0.212		0.259		0.121		0.222	Susceptibility	Susceptibility
	(°E)	(°N)	D_r	$.185D_r$	R_r	$.212R_r$	A_r	$.259A_r$	T_r	$.121T_r$	LU_r	Index (VI)	Class (SC)
1	7.4222	6.8525	7	1.295	8	1.696	8	2.072	10	1.21	50	11.1	17.373	Low
2	7.4098	6.8596	1	0.185	8	1.696	6	1.554	10	1.21	50	11.1	15.745	Low
3	7.4127	6.8693	5	0.925	8	1.696	6	1.554	10	1.21	50	11.1	16.485	Low
4	7.4231	6.8613	2	0.37	8	1.696	8	2.072	10	1.21	50	11.1	16.448	Low
5	7.3843	6.8634	3	0.555	8	1.696	6	1.554	8	0.968	50	11.1	15.873	Low
6	7.4267	6.8613	3	0.555	8	1.696	6	1.554	10	1.21	50	11.1	16.115	Low
7	7.4079	6.8691	3	0.555	8	1.696	6	1.554	10	1.21	50	11.1	16.115	Low
8	7.3586	6.8948	3	0.555	8	1.696	6	1.554	10	1.21	50	11.1	16.115	Low
9	7.4065	6.9247	7	1.295	8	1.696	6	1.554	8	0.968	50	11.1	16.613	Low
10	7.4089	6.8698	1	0.185	8	1.696	6	1.554	8	0.968	50	11.1	15.503	Low
11	7.4065	6.8585	3	0.555	8	1.696	6	1.554	8	0.968	50	11.1	15.873	Low
12	7.4056	6.8681	1	0.185	8	1.696	6	1.554	8	0.968	50	11.1	15.503	Low
13	7.4123	6.8716	2	0.37	8	1.696	6	1.554	8	0.968	50	11.1	15.688	Low
14	7.4038	6.8719	1	0.185	8	1.696	6	1.554	10	1.21	50	11.1	15.745	Low
15	7.4275	6.9493	5	0.925	8	1.696	6	1.554	8	0.968	50	11.1	16.243	Low
16	7.4105	6.8651	9	1.665	8	1.696	6	1.554	8	0.968	50	11.1	16.983	Low
17	7.4016	6.8589	5	0.925	3	0.636	6	1.554	8	0.968	50	11.1	15.183	Low
18	7.4091	6.8625	1	0.185	8	1.696	6	1.554	8	0.968	50	11.1	15.503	Low
19	7.4132	6.8639	3	0.555	8	1.696	6	1.554	10	1.21	50	11.1	16.115	Low
20	7.3980	6.8617	1	0.185	8	1.696	6	1.554	10	1.21	50	11.1	15.745	Low
21	7.4067	6.8696	2	0.37	8	1.696	6	1.554	10	1.21	50	11.1	15.93	Low
22	7.3459	6.8170	1	0.185	8	1.696	6	1.554	8	0.968	50	11.1	15.503	Low
23	7.3863	6.8676	9	1.665	8	1.696	6	1.554	8	0.968	50	11.1	16.983	Low
24	7.4635	6.8351	9	1.665	8	1.696	6	1.554	10	1.21	50	11.1	17.225	Low
25	7.4616	6.8294	2	0.37	8	1.696	6	1.554	10	1.21	50	11.1	15.93	Low
26	7.4711	6.8203	2	0.37	8	1.696	6	1.554	10	1.21	50	11.1	15.93	Low
27	7.5848	6.8216	2	0.37	8	1.696	6	1.554	10	1.21	50	11.1	15.93	Low
28	7.6068	6.8354	5	0.925	8	1.696	8	2.072	10	1.21	50	11.1	17.003	Low
29	7.5493	6.8094	1	0.185	8	1.696	6	1.554	10	1.21	50	11.1	15.745	Low
30	7.6103	6.8372	3	0.555	8	1.696	8	2.072	10	1.21	50	11.1	16.633	Low
31	7.6109	6.8351	3	0.555	8	1.696	8	2.072	10	1.21	50	11.1	16.633	Low
32	7.5991	6.8309	3	0.555	8	1.696	8	2.072	10	1.21	50	11.1	16.633	Low
33	7.5918	6.8266	3	0.555	8	1.696	8	2.072	10	1.21	50	11.1	16.633	Low
34	7.5955	6.8305	1	0.185	8	1.696	8	2.072	10	1.21	50	11.1	16.263	Low
35	7.5546	6.8089	2	0.37	8	1.696	8	2.072	10	1.21	50	11.1	16.448	Low
36	7.5596	6.8629	3	0.555	8	1.696	8	2.072	10	1.21	50	11.1	16.633	Low
37	7.5798	6.8140	5	0.925	8	1.696	8	2.072	10	1.21	50	11.1	17.003	Low
38	7.5641	6.7984	9	1.665	8	1.696	6	1.554	10	1.21	50	11.1	17.225	Low
39	7.5690	6.8023	5	0.925	8	1.696	8	2.072	10	1.21	50	11.1	17.003	Low
40	7.5266	6.8099	5	0.925	8	1.696	8	2.072	10	1.21	50	11.1	17.003	Low
41	7.5366	6.7938	3	0.555	8	1.696	6	1.554	10	1.21	50	11.1	16.115	Low
42	7.5978	6.8138	5	0.925	8	1.696	6	1.554	10	1.21	50	11.1	16.485	Low
43	7.5299	6.7810	2	0.37	8	1.696	6	1.554	10	1.21	50	11.1	15.93	Low
44	7.5763	6.7807	7	1.295	8	1.696	6	1.554	10	1.21	50	11.1	16.855	Low
45	7.6074	6.8359	3	0.555	8	1.696	6	1.554	10	1.21	50	11.1	16.115	Low
46	7.6078	6.8221	1	0.185	8	1.696	6	1.554	10	1.21	50	11.1	15.745	Low
47	7.6078	6.8070	1	0.185	8	1.696	8	2.072	10	1.21	50	11.1	16.263	Low
48	7.4901	6.8382	1	0.185	8	1.696	6	1.554	10	1.21	50	11.1	15.745	Low
49	7.6055	6.8975	3	0.555	8	1.696	8	2.072	10	1.21	50	11.1	16.633	Low
50	7.5459	6.8274	7	1.295	8	1.696	6	1.554	10	1.21	50	11.1	16.855	Low

DOI: 10.6092/issn.2281-4485/21761

ly shielding the aquifer. Materials with fine grains, such as silt or loamy soils, filter out pollutants as water moves through them, reducing contamination risks. These characteristics ensure that contaminants take longer to reach the groundwater or are attenuated along the way, contributing to the area's classification as low vulnerability. This classification highlights the area's resilience to contamination, supporting its sustainable use for drinking water and other purposes. The variation of susceptibility index is illustrated in Figure 5.

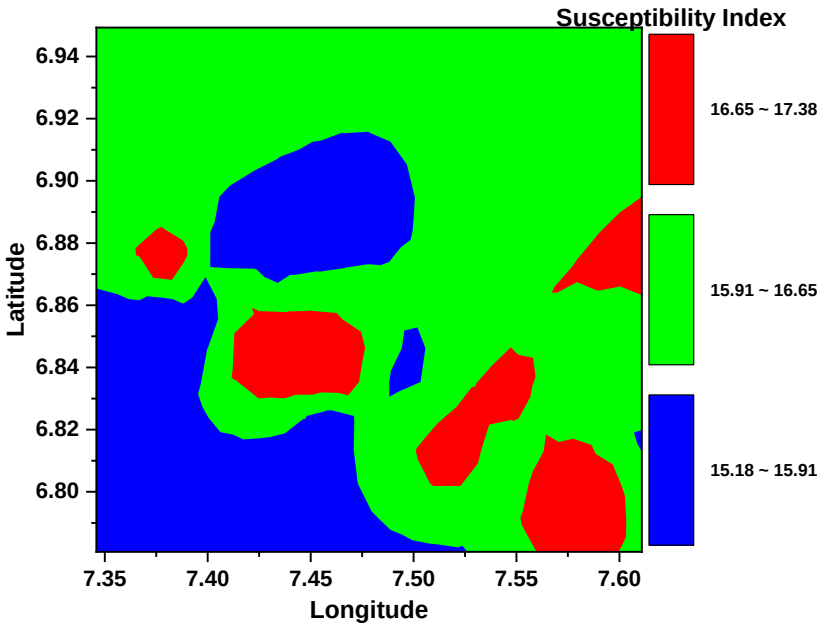

Figure 5
Contour map showing the Susceptibility index

Comparing GOD, GLSI, DRIST and SI. The comparison of the vulnerability indices reveals differing conclusions about the study area's susceptibility to contamination, each emphasizing distinct environmental factors: The GOD Index classifies the entire study area as low vulnerability. Despite this classification, there remains a risk from persistent pollutants. The low vulnerability implies fewer immediate concerns, but long-term preventive measures are still crucial. The GLSI index divides the area into low and moderate susceptibility zones, with 62% of the area classified as moderate. This reflects a mix of geological conditions offering varying degrees of protection. The moderate susceptibility zones are more prone to contamination, necessitating stricter zoning regulations. The DRIST Index also classifies the study area into low and moderate vulnerability zones, with 64% of the area being low vulnerability. It highlights the presence of natural barriers like impermeable layers that slow the infiltration of contaminants. While contamination risks in the low vulnerability zones are low, moderate zones should be subject to intensive monitoring. The SI Index classifies the entire study area as low vulnerability, similar to the GOD Index. It underscores the presence of protective layers, like clay. or dense soil, which reduce the risk of contamination. This classification supports the area's suitability for sustainable groundwater use but calls for continued vigilance through proper land-use practices.

Conclusions

The delineation of aquifer vulnerability in Eha Alumona, Nsukka Local Government Area, Enugu State, Nigeria, have revealed significant spatial variability in the subsurface geoelectric properties, highlighting the heterogeneity of the underlying geologic formations and aquifer systems. Data from fifty VES stations reveal five geoelectric layers with varying resistivity, thickness, and depth, reflecting the heterogeneity of subsurface materials. The first two layers exhibit lower resistivity values (5.7–767.2 Ωm, suggesting surface materials such as sandy soil, clay, or weathered rock, while deeper layers show a broader resistivity range (2.6–87,620.9 Ωm), indicating diverse geological compositions. The GOD index values (0.12–0.24) classify the study area as having low vulnerability, suggesting significant protection against contamination due to deep water tables, overlying impermeable overlying layers and confined or semi-confined aquifer conditions. These natural barriers reduce the risk of ra-

DOI: 10.6092/issn.2281-4485/21952

pid contaminant infiltration and migration. However, the low vulnerability classification does not preclude the possibility of contamination, especially from persistent pollutants like nitrates and pesticides, necessitating preventive measures to sustain groundwater quality. The GLSI values (1.33 – 2.67) classify the area into low (38%) and moderate (62%) susceptibility zones. Low susceptibility zones indicate high protective capacity due to compacted soils or clay layers. Moderate susceptibility zones cover the greater part of the study area and have intermediate protective capacity, with subsurface materials that may include sandy loam or mixed lithology. The DRIST index values (89 – 143) delineate the study area into low (64%) and moderate (36%) vulnerability zones. Low vulnerability zones, observed in the northeastern and southwestern parts of the study area, are well-protected by impermeable layers or deeper water tables. Moderate vulnerability zones are more prone to contamination due to factors such as moderately permeable soils and higher recharge rates. The SI index (15.503 – 17.373) categorizes the study area as having low vulnerability. This reflects the aquifer's strong natural protection which may be due to deep-water table, low recharge rates, and the presence of impermeable materials like clay and silt. These conditions minimize contaminant infiltration and enhance groundwater resilience, making the aquifer suitable for sustainable use. In conclusion, the study highlights the interplay of geological and hydrological factors in determining aquifer vulnerability in Eha Alumona. With proper management, the area's groundwater resources can be protected and sustainably utilized for future needs.

Acknowledgements

The authors are grateful to the Atmospheric and Solid Earth Geophysics Research Group of the University of Nigeria, Nsukka.

Conflict of interest

The authors declare that they have no conflict of interest.

References

AGAGU O.K., FAYOSE E.A., PATERS S.W. (1985) Stratigraphy and sedimentation in the Senonian Anambra basin of Eastern Nigeria. Journal of Mining and Geology, 2: 25–35.

ALLER L., LEHR J. H., PETTY R., BENNETT T. (1987) DRASTIC: A standardized system to evaluate ground water pollution potential using hydrogeologic settings. In Petroleum hydrocarbons and organic chemicals in ground water: Prevention, detection and restoration (pp. 38–57).

BABIKER I.S., MOHAMED M.A.A., HIYAMA T., KATO K. (2005) A GIS-based DRASTIC model for assessing aquifer vulnerability in Kakamigahara Heights, Gifu Prefecture, central Japan. Science of the Total Environment, 345(1–3):127–140.

BAKTI H., LUBIS R.F., DELINOM R.M., TANIGUCHI M. (2017) Submarine groundwater discharge (SGD) measurement on the sandy unconfined aquifer in the Carnaval Beach-Ancol Jakarta Bay. Marine Research in Indonesia, 41(2):59–65. https://doi.org/10.14203/mri.v41i2.110

BANERJEE A., CREEDON L., JONES N., GILL L., GHARBIA S. (2023) Dynamic groundwater contamination vulnerability assessment techniques: A systematic review. Hydrology, 10: 182. https://doi.org/10.3390/hydrology10090182

BARBULESCU A. (2020) Assessing groundwater vulnerability: DRASTIC and DRASTIC-like methods: A review. Water, 12:1356. https://doi.org/10.3390/w12051356

BRINDHA K., ELANGO L. (2015). Cross comparison of five popular groundwater pollution vulnerability index approaches. Journal of Hydrology, 524: 597–613. https://doi.org/10.1016/j.jhydrol.2015.03.003

FOSTER S.D. (1987) Fundamental concepts in aquifer vulnerability, pollution risk, and protection strategy. In W. Van Duijvenbooden & H. G. Van Waegeningh (Eds.), Vulnerability of soil and groundwater to pollutants (69–86).

GEORGE N.J., EKANEM A.M., THOMAS J.E., UDOSEN N.I., OSSAI N.M., ATAT J.G. (2023) Electrosequence valorization of specific enablers of aquifer vulnerability and contamination: A case of index-based model approach for ascertaining the threats to quality groundwater in sedimentary beds. HydroResearch. https://doi.org/10.1016/j.hydres.2023.11.006

GHOUILI N., JARRAYA-HORRICHE F., HAMZAOUI-AZAZA F., ZAGHRARNI M.F., RIBEIRO L. ZAMMOURI M. (2021). Groundwater vulnerability mapping using the Susceptibility Index (SI) method: Case study of Takelsa aquifer, Northeastern Tunisia, Journal of African Earth Sciences, 178: 104035. https://doi.org/10.1016/j.jafrearsci.2020.104035

HILAL I., OUBEID A.M., QURTOBI M., AQNOUY M., AMENZOU N., SAADI R., RAIBI F., BELLARBI M., SI MHAMDI H., SADIKI M., HASNAOUI M.D., BENMANSOUR M. (2024) Groundwater vulnerability mapping using the susceptibility index (SI) method and tritium isotopes: A case study of the Gharb aquifer in northwestern Morocco. E3S Web of Conferences 489: 07001. ttps://doi.org/10.1051/e3sconf/202448907001

DOI: 10.6092/issn.2281-4485/21952

IBUOT J.C., OBIORA D.N., EKPA M.M., OKOROH D. O. (2017) Geoelectrohydraulic investigation of the surficial aquifer units and corrosivity in parts of Uyo L. G. A., Akwa Ibom State, Southern Nigeria. Applied Water Science, 7: 4705–4713.

IBUOT J.C., GEORGE N.J., OKWESILI A.N., OBIORA D.N. (2019a) Investigation of litho-textural characteristics of aquifer in Nkanu West Local Government Area of Enugu state, southeastern Nigeria. Journal of African Earth Sciences, 157:197–207.

IBUOT J.C., OKEKE F.N., OBIORA D.N. GEORGE N. J. (2019b) Assessment of impact leachate on hydrogeological repositories in Uyo, Southern Nigeria. Journal of Environmental Engineering and Science, 14(2): 97-107.

IBUOT J.C., OBIORA D.N., EKPA M.M., OMEJE E.T. (2024) Geo-electric techniques for estimating and mapping the electro-geohydraulic properties of the shallow aquifer within the Nsukka Formation in eastern Nigeria. Earth Sciences Research Journal, 28(3):349–359. https://doi.org/10.15446/esrj.v28n3.110328

IFEDIEGWU S.I., CHIBUIKE I.E. (2021) GIS-based evaluation of shallow aquifer vulnerability to pollution using DRASTIC model: A case study on Abakaliki, southeastern Nigeria. Arabian Journal of Geosciences, 14: 2534. https://doi.org/10.1007/s12517-021-08811-8

KAGABU M., DELINOM R.M., LUBIS R.F., SHIMADA J., TANIGUCHI M. (2010) Groundwater characteristics in Jakarta area, Indonesia. Jurnal RISET Geologi dan Pertambangan, 20(2): 69. https://doi.org/10.14203/risetgeotam2010.v20.35

KHEMIRI S., KHNISSI A., ALAYA B.A., SAIDI S., ZARGROUNI F. (2013) Using GIS for the comparison of intrinsic parameter methods assessment of groundwater vulnerability to pollution in scenarios of semiarid climate: The case of Foussana groundwater in the central of Tunisia. Journal of Water Resource and Protection, 5(8), 835–845.

KIRLAS M.C., KARPOUZOS D.K., GEORGIOU P.E., KATSIFARAKIS K.L. (2022) A comparative study of groundwater vulnerability methods in a porous aquifer in Greece. Applied Water Science, 12: 123. https://doi.org/10.1007/s13201-022-01651-1

LASHKARIPOUR G.R., NAKHAEI M. (2005) Geoelectrical investigation for the assessment of groundwater conditions: A case study. Annales Geophysicae, 48(6):937–944.

LOKE M.H. (2009) Electrical imaging surveys for environmental and engineering studies: A guide to 2D and 3D surveys. Workshop held at USM.

MANSOUR K., OMAR K., ALI K., ABDEL ZAHER M. (2018) Geophysical characterization of the role of fault and fracture systems for recharging groundwater aquifers from surface water of Lake Nasser. NRIAG Journal of Astronomy and Geophysics, 7(1):99–106. https://doi.org/10.1016/j.nrjag.2018.02.001

NEJATIJAHROMI Z., NASSERY H.R., HOSONO T., NAKHAEI M., ALIJANI F., OKUMURA A. (2019) Groundwater nitrate contamination in an area using urban wastewaters for agricultural irrigation under arid climate condition, southeast of Tehran, Iran. Agricultural Water Management, 221:397–414.

NUGRAHA G.U., BAKTI H., LUBIS R.F., SUDRAJAT Y., ARISBAYA I. (2021) Aquifer vulnerability in the coastal northern part of Lombok Island, Indonesia. Environment, Development and Sustainability, 24:1390–1410.

OBAJE N.G. (2009) Geology and mineral resources of Nigeria (Vol. 120). Springer.

OBIORA D.N., IBUOT J.C. (2020) Geophysical assessment of aquifer vulnerability and management: A case study of University of Nigeria, Nsukka, Enugu State. Applied Water Science, 10:29. https://doi.org/10.1007/s13201-019-1113-7

OGBUKAGU I.N. (1976) Soil erosion in the northern parts of Awka—Orlu uplands Nigeria. Journal of Mining and Geology, 13(2):6–19.

OMEJE E.T., IBUOT J.C., UGBOR D.O., OBIORA D.N. (2022) Geophysical investigation of transmissibility and hydrogeological properties of aquifer system: A case study of Edem, Eastern Nigeria. Water Supply, 22(5):5044–5055.

OMEJE E.T., OBIORA D.N., OKEKE F.N., IBUOT J.C., OMEJE V.D. (2023a) Application of geoelectric technique and sensitivity analysis in assessment of aquifer vulnerability: A case study of Nsukka and Igbo Etiti area, Eastern Nigeria. Environment, Development and Sustainability. https://doi.org/10.1007/s10668-023-03351-5

OMEJE E.., OBIORA D.N., OKEKE F.N., IBUOT J.C., UGBOR D.O. (2023b) Investigation of aquifer vulnerability and sensitivity analysis of modified DRASTIC and SINTACS models: A case study of Ovogovo Area, Eastern Nigeria. Acta Geophysica. https://doi.org/10.1007/s11600-022-00992-4

ONI T.E., OMOSUYI G.O., AKINLALU A.A. (2017) Groundwater vulnerability assessment using hydrogeologic and geoelectric layer susceptibility indexing at Igbara Oke, Southwestern Nigeria. NRIAG Journal of Astronomy and Geophysics, 6(2): 452–458. https://doi.org/10.1016/j.nrjag.2017.04.009

PATEL P., MEHTA D., SHARMA N. (2022) A review on the application of the DRASTIC method in the assessment of groundwater vulnerability. Water Supply, 22:5–5190. https://doi.org/10.2166/ws.2022.126

DOI: 10.6092/issn.2281-4485/21952

PISCOPO G. (2001). Groundwater vulnerability map explanatory notes – Castlereagh Catchment. NSW Department of Land and Water Conservation, Parramatta, NSW, Australia.

PUTRANTO T.T., HIDAJAT W.K., SUSANTO N. (2017) Developing groundwater conservation zone of unconfined aquifer in Semarang, Indonesia. IOP Conference Series: Earth and Environmental Science, 55:01036.

PUTRANTO T.T., SANTI N., DIAN AGUS, WIDIARSO, D. A., DIMAS P. (2018). Application of aquifer vulnerability index (AVI) method to assess groundwater vulnerability to contamination in Semarang urban area. MATEC Web of Conferences, 159, 01036.

RAHMAN A.A. (2008) GIS-based DRASTIC model for assessing groundwater vulnerability in shallow aquifer in Aligarh, India. Applied Geography, 28:32–53. https://doi.org/10.1016/j.apgeog.2007.07.008

REYMENT R.A. (1965). Aspects of the geology of Nigeria. Ibadan University Press.

RUSYDI A.F., NAILY W., LESTIANA H. (2015) Pencemaran limbah domestik dan pertanian terhadap air tanah bebas di kabupaten Bandung. Jurnal RISET Geologi dan Pertambangan, 25(2):87. https://doi.org/10.14203/risetgeotam2015.v25.201

SARAVANAN S.T. (2021) Evolution of a hybrid approach for groundwater vulnerability assessment using hierarchical fuzzy DRASTIC models in the Cuddalore region, India. Environmental Earth Science, 80(5):1–25.

SARAVANAN S., PARTHASARATHY K.S.S., SIVARANJANI S. (2018) Assessing coastal aquifer to seawater intrusion: Application of the GALDIT method to the Cuddalore aquifer, India. In Global perspectives, regional processes, local issues. Elsevier. https://doi.org/10.1016/B978-0-12-814350-6.00010-0

STEMPVOORT D.V., EWERT L., WASSENAAR L. (1993) Aquifer vulnerability index: A GIS-compatible method for groundwater vulnerability mapping. Canadian Water Resources Journal, 18(1), 25–37.

STIGTER T.Y., RIBEIRO L., CARVALHO A.M.M., DILL D. (2006) Evaluation of an intrinsic and a specific vulnerability assessment method in comparison with groundwater salinization and nitrate contamination levels in two agricultural regions in the south of Portugal. Hydrogeology Journal, 14(1–2):79–99. https://doi.org/10.1007/s10040-004-0396-3

SULTANA Q., SULTANA A. (2024). Groundwater pollution and its assessment: A review. 4th International Symposium of Scientific Research and Innovative Studies (ISSRIS'24).

TEIXEIRA J., CHAMINÉ H.I., ESPINHA MARQUES J., CARVALHO J.M., PEREIRA A.J.S.C., CARVALHO M. R., FONSECA P.E., PÉREZ-ALBERTI A., ROCHA F. (2015) A comprehensive analysis of groundwater resources using GIS and multicriteria tools (Caldas Da Cavaca, Central Portugal): Environmental issues. Environmental Earth Sciences, 73(6):2699–2715. https://doi.org/10.1007/s12665-014-3602-1

TRESOLDI G., AROSIO D., HOJAT A., LONGONI L., PAPINI M., ZANZI L. (2019) Long-term hydrogeophysical monitoring of the internal conditions of river levees. Engineering Geology, 259:105139. https://doi.org/10.1016/j.enggeo.2019.05.016

UGWUANYI M.C., IBUOT J.C., OBIORA D N. (2015) Hydrogeophysical study of aquifer characteristics in some parts of Nsukka and Igbo Eze south local government areas of Enugu State, Nigeria. International Journal of Physical Sciences, 10(15):425–435.

YUSUF M. A., ABIYE T.A. (2019) Risks of groundwater pollution in the coastal areas of Lagos, southwestern Nigeria. Groundwater for Sustainable Development. https://doi.org/10.1016/j.gsd.2019.100222

ZHAI Y., ZHAO X., TENG Y., LI X., ZHANG J., WU J., ZUO R. (2017) Groundwater nitrate pollution and human health risk assessment by using HHRA model in an agricultural area, NE China. Ecotoxicology and Environmental Safety. https://doi.org/10.1016/j.ecoenv.2016.11.010